ChemPubSoc Europe

DOI: 10.1002/open.202000041

Open Access ChemistryOPEN Full Papers

Special Collection

Interfacial Synthesis of a Monolayered Fluorescent Two-Dimensional Polymer through Dynamic Imine Chemistry

Zhaohui Zhang,[a] Hui Liu,[a] Qingzhu Sun,[a] Feng Shao,[b] Qingyan Pan,[a] Tao Zhuang,*[a] and Yingjie Zhao*[a]

A fluorescent monolayered two-dimensional polymer (2DP) containing both tetraphenylethylene (TPE) and imine linkages is synthesized at air-water interface using the Langmuir-Blodgett method. We designed TPE-based monomers with long distances between the TPE and the imine linkages to avoid the charge transfer and therefore keep the fluorescence. A monolayered 2DP provided with more than 104 μm^2 in domain size and around 0.8 nm thickness was obtained through a successive Schiff base reaction at air-water interface. The nanostructures and fluorescent property of 2DP films were characterized by optical microscopy, SEM, TEM, AFM and fluorescence spectrum. Most importantly, the tip-enhanced Raman spectroscopy (TERS) was utilized here to confirm the success of the polycondensation of monolayered 2DP.

1. Introduction

Two-dimensional polymers (2DPs) have been generally accepted as materials with atomic-thick or monolayer, covalently linked, highly ordered 2D topological network.[1–8] The recent high interest and the fast development of 2DPs materials are driven by their unique structures,[9–11] potential applications[12–16] and infinite structure possibilities through monomer design.[17] The properties of the 2DPs are completely different from those of traditional linear or branched polymers due to the total different 2D structure. The structure change from 1D to 2D at the molecular level is particularly interesting and promising for applications in optoelectronic devices,[18–21] energy conversion,[22,23] sensors,[24–26] and biomimetic devices.[27–29] In addition, the 2D, ultrathin and porous natures of the 2DPs are efficiently utilized in osmotic energy conversion, also demonstrating high-performance power capture by mixing artificial river water and sea water.[30–32] Therefore, the 2DPs provide new prospects of potential applications in promising fields such as the salinity gradient energy conversion and ion screening.[33–35] Nevertheless, the synthesis of the 2DPs is usually challenging, especially the monolayer synthesis. So far, several strategies have been developed such as single crystal to single crystal method,[36–38] solution synthesis,[11,39] and interfacial synthesis.[40–43] Among which the interfacial synthesis method is ideal to obtain ultrathin, large-area, free-standing 2DPs under ambient conditions. In this process, polymerization of monomers takes place directly at the interface of two phases and ends up with mono- or few- layered 2DPs. Several pioneering researches have been conducted by using different reactions such as Schiff base,[40,43–45] [4+4] cycloaddition,[41,42,46–48] and Glaser-Hay coupling reaction.[49–51] Among these reactions, dynamic imine chemistry at the air/water interface (Langmuir-Blodgett method)[40,44,52,53] has great potential for large-scale production of highly crystalline 2D polymers due to its dynamic self-healing process. In addition, with certain functional moieties embedded into the well-defined 2DPs, the resulting 2DPs materials can possess unique properties for specific application. Tetraphenylethene (TPE),[54–57] as a star molecule of classical aggregation-induced emission (AIE) effect has been demonstrated to be an excellent moiety for constructing luminescent materials such as chemosensors,[58,59] bio-probes,[60] optical devices[61–63] and so on because of their excellent luminescent properties and unique superiority compared with conventional aggregation-caused quenching (ACQ) effect. However, owing to the shortage of a suitable linkage that combines stability with luminescence, most of the 2D networks containing TPE units are less luminescent.[64–66] For example, the mostly used dynamic imine chemistry for construct 2D network based TPE is non-fluorescent because the charge transfer between the lone pair electrons from the imine to the fluorescent TPE.[64,65,67] Recently, we reported a highly fluorescent 2DP films based on TPE unis by using conjugated diyne or host-guest supramolecular interactions as linkages.[10,68] Beside, boronate and boroxine linkages can also form luminescent 2D frameworks based on TPE, but they are unstable under protic conditions or upon exposure to air.[69] Developing an imine linked fluorescent 2DP films based on TPE units remains challenging. In this work, we designed a TPE-based monomers with long distances between the TPE and the imine linkages.

[a] Z. Zhang, H. Liu, Q. Sun, Q. Pan, Prof. T. Zhuang, Prof. Y. Zhao
College of Polymer Science and Engineering
Qingdao University of Science and Technology
Qingdao 266042 (China)
E-mail: yz@qust.edu.cn
zhuangtao1234@126.com

[b] F. Shao
Department of Chemistry, Faculty of Science, National University of Singapore, 3 Science Drive 3, Singapore 117543.

Supporting information for this article is available on the WWW under https://doi.org/10.1002/open.202000041

Special Collection An invited contribution to a Special Collection dedicated to Functional Supramolecular Systems

The charge transfer between the imine and TPE was inhibited and the fluorescence maintained. A monolayered fluorescent 2DP containing both TPE and imine linkage was obtained at the air-water interface. The imine-linked chemical structure of the obtained monolayer was further analyzed by tip-enhanced Raman spectroscopy (TERS) which has been proved to be an attractive method for analyzing monolayered 2DP as this technology contains both the spatial resolution of the scanning probe microscopes and the chemical selectivity of traditional Raman spectroscopy.[40,47,70–72]

2. Results and Discussion

The synthesis of monomer **3** was based on Sonogashira reaction between compound 1,1,2,2-tetrakis(4-ethynylphenyl) ethene and 4-iodobenzaldehyde (Scheme S1). The imine-linked 2DP films were synthesized from two simple aromatic building blocks: p-phenylenediamine (**4**) and 4,4′,4″,4‴-((ethene-1,1,2,2-tetrayltetrakis(benzene-4,1-diyl))tetrakis(ethyne-2,1-diyl))tetrabenzaldehyde (**3**) (Figure 1). At the air/water interface, relatively large molecule extended by benzene ring and alkynyl group could be well spreaded. The benzene ring and alkynyl group between the TPE and imine-linkage could better prevent the photo induced electron transfer (PET) from the imine to the TPE and thus the fluorescence maintains. Such a conformation would render **3** a good candidate for the interfacial synthesis of the fluorescent polyimine monolayer. Ideally, strain-free imine linkages will be formed between the tetraaldehyde and diamine follow-through orient themselves. The reversible imine bond could enable selfmodification, correct the formations of undesirable bond to produce a thermodynamically favorable polymer product with a highly ordered structure in the end.

The monolayer 2DP films was prepared at the air-water interface of a Langmuir-Blodgett (LB) trough. Figure 1 illustrates the interfacial synthesis process of the 2DP films by Schiff-base polycondensation. 50 μl chloroform solution of monomer **3** (1.2×10^{-3} mM) was first spreaded at the air-water interface of the LB trough and then compressed to a surface pressure of 25 mN m^{-1}, which would facilitate the formation of densely packed monomer **3** (Figure S4). Afterwards, 75 μl solution of momomer **4** in water (1.3×10^{-3} mM) was added to the subphase and allowed to diffused to the interface slowly where the polymerization was triggered by the formation of imine bonds between amine and aldehyde. Acetic acid (0.35 mL) was then injected slowly into the solution without disturbing the self-assembled monomer layer. The system was kept undisturbed overnight. The resulting polymer sheet could be easily transferred onto 300 nm SiO_2/Si silicon wafers or TEM grids by using horizontal Schäfer-type transfer method for further characterization.[41,42,73]

The polymerization at interface of Langmuir trough resulted in a large-area, freestanding film with a size of square millimeter (Figure 2a). Obvious cracks can be seen under optical microscope (OM) (Figure 2a). The morphology of the 2DP film was further investigated by scanning electron microscopy (SEM), transmission electron microscopy (TEM), HR-TEM and atomic force microscopy (AFM). The SEM, TEM and HR-TEM images (Figure 2b, c, d) show clear thin films morphology. The SEM image (Figure 2b) of the homogenous film on a silicon wafers illustrates that even area with more than 400 μm^2 were fully spanned. The sample on the grids for TEM are stable under electron-beam irradiation and do not burn immediately when the beam is focused. HR-TEM images fail to verify their lattice data. Atomic force microscopy (AFM) confirms that the polyimine film is a monolayer (Figure 2e). An average thickness of the 2DP films is about 0.8 nm[40] after calculating more than 20 points measured from 5 different samples with smooth surface over large areas.

TERS spectra further confirmed the successful formation of the polyimide based on Schiff-base polycondensation. Contained the superiorities of Raman spectroscopy with scanning probe microscopy (SPM), the chemical fingerprint and topography of monolayered 2DP films are recorded synchronously

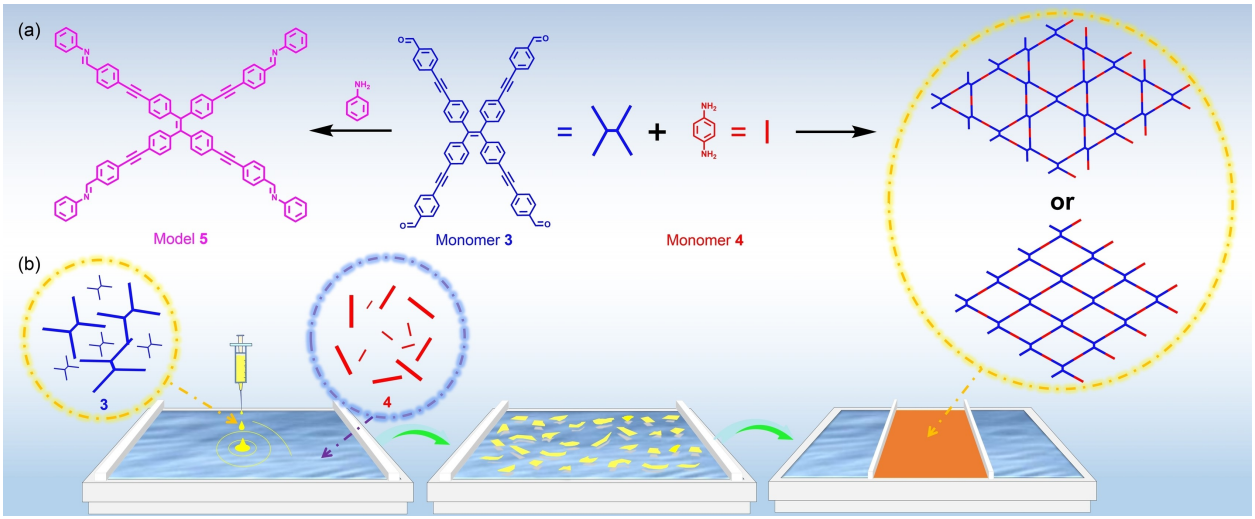

Figure 1. (a) Scheme of the synthesis route and topological structure of the 2DP films. (b) Schematic illustration of the experimental process.

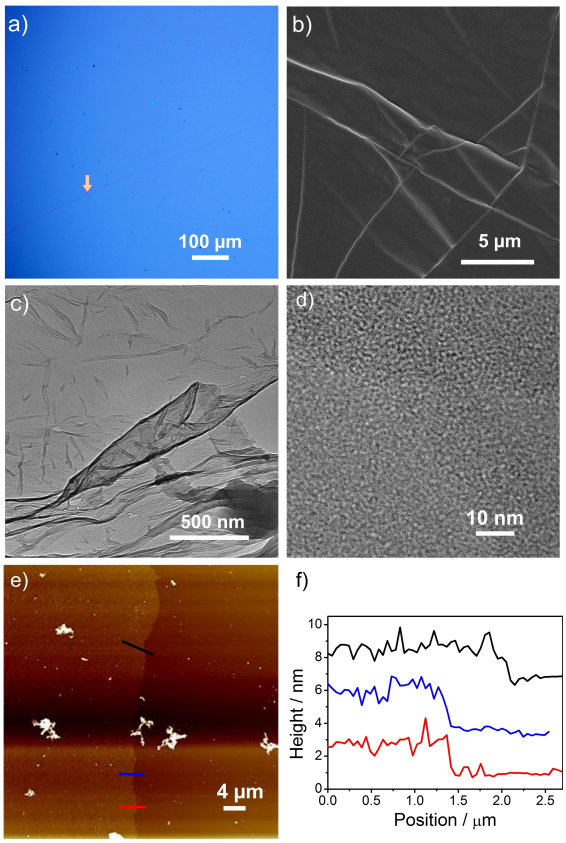

Figure 2. (a) OM image on 300 nm SiO_2/Si; (b) SEM image; (c) TEM image; (d) HR-TEM image; (e) AFM image on SiO_2/Si; (f) cross-sectional analysis along the black, blue and red line of the obtained in (e).

by TERS with nanoscale resolution.[61,62] Moreover, TERS has been testified to provide single molecule sensitivity,[74,75] which is essential for gaining Raman signals of a monolaylered 2DP films. In order to acquire preliminary understanding about the chemical structure of the obtained films, the 2DP monolayer and corresponding finite model **5** (Figure 1) were characterized by TERS (Figure 3), verified by more than 20 spots discretionarily selected from different sheet samples. Simultaneously, monomer **3**, **4** and model **5** as references were also investigated by confocal Raman spectroscopy by measuring variations in the intensity of the bands corresponding to vibrations of the CHO, NH_2, C=N, and C≡C groups (Figure 3).

After Schiff-base condensation in model **5**, the band of aldehyde C=O stretching mode (1706.7 cm^{-1}) in monomer **3** and the band of diamine NH_2 wagging mode (1394.3 cm^{-1}) in monomer **4** are absent in the Raman spectra. Meanwhile, new peaks at 1623.7 and 1648.3 cm^{-1} exhibit in the TERS and confocal Raman spectra of model **5** and 2DP films, respectively, which are caused by the stretching vibrations of the C=N group from the imine. This clearly indicates the formation of the proposed imine bonds in the 2DP films and model **5**. Additionally, the slight blue shift of the C=N bonds in 2DPs (1648.3 cm^{-1}) compared to model **5** (1623.7 cm^{-1}) arise from the change of molecular orientations on the metallic surface.[34,61] It is particularly noteworthy that the alkyne C≡C

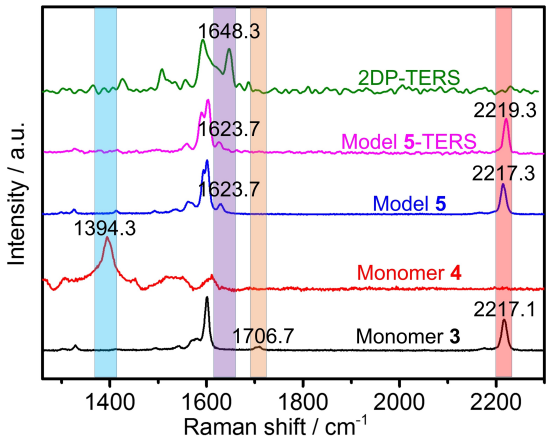

Figure 3. Confocal Raman spectra of the monomer **3** (black), monomer **4** (red) and model **5** (blue) on 300 nm SiO_2/Si; Tip-enhanced Raman spectra of 2DP films (green) and Model **5** (pink) on 50 nm gold coated microscope slide.

(2217.1 cm^{-1}) peak of the 2DP films, compared to imine model **5**, has disappeared in the TERS spectrum, which is due to the surface selection rules for C≡C bonds on metallic substrates.[61,62] This fact further confirms the formation of 2D polyimine networks, leading to integrated monomer **3** forcibly lying on the substrate.[61,62]

The photophysical property of the 2DP was then studied. Beside the evidence from the change of TERS, the fluorescence before and after the polymerization is also different. The single layer of the monomer and 2DP films samples were smoothly impregnated with quartz plate ($\Phi = 1$ cm). The samples were analyzed by UV-vis absorbance and fluorescence spectra. The UV-vis (Figure S6) of the monomer **3** and 2DP films both exhibited an absorption range ($\lambda = 275–450$ nm). More interestingly, fluorescence spectrum of the 2DP films showed a fluorescence peak at $\lambda = 545$ nm which is significantly red-shifted (20 nm) compared to the monolayer of monomer **3** ($\lambda = 525$ nm) (Figure 4). Meanwhile, the fluorescence spectra intensity of the 2DP films decreased compared to the monomer **3** which also suggested that the polymerization was achieved.

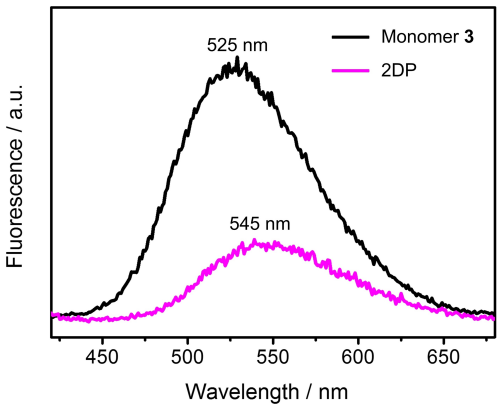

Figure 4. Fluorescence spectras of a compressed monolayer of monomer **3** at the interface and 2DP after 12 hours reaction under ambient conditions.

Still, the fluorescent characteristic of the TPE in the imine based 2DP monolayer was maintained. For comparison, the fluorescence of two fluorescent intermediates (**1**, **2**) during the synthesis of the monomer containing TPE were also measured. Figure S7 showed similar fluorescent intensities compared with the monomer **3** and slight blue shift (20 nm).

3. Conclusions

The monolayered fluorescent two-dimensional polymer containing both TPE and imine linkage was obtained on an air-water interface (Langmuir-Blodgett method). BAM imaging obtained the Langmuir-Blodgett compression shows that homogeneous monomer films can be prepared. In the meantime, the monolayered 2DP film was characterized by optical microscopy, SEM, TEM, AFM, and TERS. Image representation obtained by optical microscopy, SEM, TEM and AFM shows that the monolayered fluorescent 2DP films possesses the structure of such smooth, coherent, large, and freestanding polyimine monolayers yielding large surface areas (104 μm^2 in domain size) and average thickness of 0.9 nm. Further more, the 2DP film that still has a certain strength after the completion of the polymerization is rare. Although the molecular structure of the single-deck 2DP films cannot yet be uncovered by using imaging techniques such as TEM, we found that TERS ramanbased evidence for the existence of imine bonds in combination with the AFM-determined sheet thickness showing the monolayer property provides strong basis for the proposed structure.

Supporting Information

Supporting Information is available from the Wiley Online Library or from the author.

Acknowledgements

Z.Z. and H.L. contributed equally to this work. This work was supported by the National Natural Science Foundation of China (21604046), the National Young Thousand Talents Program, Shandong Provincial Natural Science Foundation, China (ZR2016XJ004).

Conflict of Interest

The authors declare no conflict of interest.

Keywords: 2D polymers · dynamic chemistry · interfacial synthesis · supramolecular assembly · aggregation induced emission

[1] J. Azadmanjiri, J. Wang, C. C. Berndt, A. M. Yu, *J. Mater. Chem. A* **2018**, *6*, 3824–3849.
[2] S. Clair, D. G. de Oteyza, *Chem. Rev.* **2019**, *119*, 4717–4776.
[3] J. W. Colson, W. R. Dichtel, *Nat. Chem.* **2013**, *5*, 453–465.
[4] R. H. Dong, T. Zhang, X. L. Feng, *Chem. Rev.* **2018**, *118*, 6189–6235.
[5] X. L. Feng, A. D. Schluter, *Angew. Chem. Int. Ed.* **2018**, *57*, 13748–13763.
[6] H. Liu, X. N. Kan, C. Y. Wu, Q. Y. Pan, Z. B. Li, Y. J. Zhao, *Chin. J. Polym. Sci.* **2017**, *36*, 425–444.
[7] H. Wang, Z. T. Zeng, P. Xu, L. S. Li, G. M. Zeng, R. Xiao, Z. Y. Tang, D. L. Huang, L. Tang, C. Lai, D. N. Jiang, Y. Liu, H. Yi, L. Qin, S. J. Ye, X. Y. Ren, W. W. Tang, *Chem. Soc. Rev.* **2019**, *48*, 488–516.
[8] J. Pang, R. G. Mendes, A. Bachmatiuk, L. Zhao, H. Q. Ta, T. Gemming, H. Liu, Z. Liu, M. H. Rummeli, *Chem. Soc. Rev.* **2019**, *48*, 72–133.
[9] C. Liu, E. Park, Y. Jin, J. Liu, Y. Yu, W. Zhang, S. Lei, W. Hu, *Angew. Chem. Int. Ed.* **2018**, *57*, 8984–8988.
[10] H. Liu, Z. Zhang, C. Wu, Q. Pan, Y. Zhao, Z. Li, *Small* **2018**, *15*, 1804519.
[11] Y. J. Zhao, H. Liu, C. Y. Wu, Z. H. Zhang, Q. Y. Pan, F. Hu, R. M. Wang, P. W. Li, X. W. Huang, Z. B. Li, *Angew. Chem. Int. Ed.* **2019**, *58*, 5376–5381.
[12] J. Artz, *Chemosensors* **2018**, *10*, 1753–1771.
[13] K. Dey, M. Pal, K. C. Rout, H. S. Kunjattu, A. Das, R. Mukherjee, U. K. Kharul, R. Banerjee, *J. Am. Chem. Soc.* **2017**, *139*, 13083–13091.
[14] K. J. Yu, S. Bi, W. Y. Ming, W. W. Wei, Y. H. Zhang, J. S. Xu, P. R. Qiang, F. Qiu, D. Q. Wu, F. Zhang, *Polym. Chem.* **2019**, *10*, 3758–3763.
[15] J. H. Sun, A. Klechikov, C. Moise, M. Prodana, M. Enachescu, A. V. Talyzin, *Angew. Chem. Int. Ed.* **2018**, *57*, 1034–1038.
[16] L. Mei, W. q Shi, Z. f Chai, *Bull. Chem. Soc. Jpn.* **2018**, *91*, 554–562.
[17] C. Pigot, F. Dumur, *Materials* **2019**, *12*, 662.
[18] S. Chen, G. Shi, *Adv. Mater.* **2017**, *29*, 1605448.
[19] J. Hu, L. Yan, W. You, *Adv. Mater.* **2018**, *30*, 1802041.
[20] S. Kansara, P. D. Bhuyan, Y. Sonvane, S. K. Gupta, *J. Mater. Sci.* **2019**, *54*, 11878–11888.
[21] H. Li, H. Hu, C. Bai, C. Bao, F. Guo, Z. Feng, Y. Liu, *RSC Adv.* **2019**, *9*, 7464–7468.
[22] Y. Chen, G. Jia, Y. Hu, G. Fan, Y. H. Tsang, Z. Li, Z. Zou, *Sustainable Energy Fuels* **2017**, *1*, 1875–1898.
[23] X. L. Zhang, L. Wang, L. Chen, X. Y. Ma, H. X. Xu, *Chin. J. Polym. Sci.* **2019**, *37*, 101–114.
[24] G. Das, B. P. Biswal, S. Kandambeth, V. Venkatesh, G. Kaur, M. Addicoat, T. Heine, S. Verma, R. Banerjee, *Chem. Sci.* **2015**, *6*, 3931–3939.
[25] T. Kim, Y. Kim, S. Park, S. Kim, H. Jang, *Chemosensors* **2017**, *5*, 15.
[26] C. M. Yang, T. C. Chen, Y. C. Yang, M. Meyyappan, *RSC Adv.* **2019**, *9*, 23343–23351.
[27] P. Labroo, Y. Cui, *Biosens. Bioelectron.* **2013**, *41*, 852–856.
[28] C. Tan, P. Yu, Y. Hu, J. Chen, Y. Huang, Y. Cai, Z. Luo, B. Li, Q. Lu, L. Wang, Z. Liu, H. Zhang, *J. Am. Chem. Soc.* **2015**, *137*, 10430–10436.
[29] M. Xiao, S. Wei, Y. Li, J. Jasensky, J. Chen, C. L. Brooks, Z. Chen, *Chem. Sci.* **2018**, *9*, 1769–1773.
[30] I. Gadwal, G. Sheng, R. L. Thankamony, Y. Liu, H. F. Li, Z. P. Lai, *ACS Appl. Mater. Interfaces* **2018**, *10*, 12295–12299.
[31] Q. Lyu, S. Sun, C. Li, S. Hu, L. C. Lin, *ACS Appl. Mater. Interfaces* **2018**, *10*, 18778–18786.
[32] D. B. Shinde, G. Sheng, X. Li, M. Ostwal, A. H. Emwas, K. W. Huang, Z. P. Lai, *J. Am. Chem. Soc.* **2018**, *140*, 14342–14349.
[33] P. Paletti, R. Yue, C. Hinkle, S. K. Fullerton-Shirey, A. Seabaugh, *NPJ 2D Mater. Appl.* **2019**, *3*, 19.
[34] K. Raidongia, J. Huang, *J. Am. Chem. Soc.* **2012**, *134*, 16528–16531.
[35] X. Zhu, Y. Zhou, J. Hao, B. Bao, X. Bian, X. Jiang, J. Pang, H. Zhang, Z. Jiang, L. Jiang, *ACS Nano* **2017**, *11*, 10816–10824.
[36] P. Kissel, D. J. Murray, W. J. Wulftange, V. J. Catalano, B. T. King, *Nat. Chem.* **2014**, *6*, 774–778.
[37] M. J. Kory, M. Wörle, T. Weber, P. Payamyar, S. W. van de Poll, J. Dshemuchadse, N. Trapp, A. D. Schlüter, *Nat. Chem.* **2014**, *6*, 779–784.
[38] R. Z. Lange, G. Hofer, T. Weber, A. D. Schlüter, *J. Am. Chem. Soc.* **2017**, *139*, 2053–2059.
[39] T. Y. Zhou, F. Lin, Z. T. Li, X. Zhao, *Macromolecules* **2013**, *46*, 7745–7752.
[40] W. Dai, F. Shao, J. Szczerbinski, R. McCaffrey, R. Zenobi, Y. Jin, A. D. Schlüter, W. Zhang, *Angew. Chem. Int. Ed.* **2016**, *55*, 213–217.
[41] D. J. Murray, D. D. Patterson, P. Payamyar, R. Bhola, W. Song, M. Lackinger, A. D. Schlüter, B. T. King, *J. Am. Chem. Soc.* **2015**, *137*, 3450–3453.
[42] P. Payamyar, K. Kaja, C. Ruiz-Vargas, A. Stemmer, D. J. Murray, C. J. Johnson, B. T. King, F. Schiffmann, J. Vandevondele, A. Renn, S. Gotzinger, P. Ceroni, A. Schütz, L. T. Lee, Z. Zheng, J. Sakamoto, A. D. Schlüter, *Adv. Mater.* **2014**, *26*, 2052–2058.

[43] H. Sahabudeen, H. Qi, B. A. Glatz, D. Tranca, R. Dong, Y. Hou, T. Zhang, C. Kuttner, T. Lehnert, G. Seifert, U. Kaiser, A. Fery, Z. Zheng, X. Feng, *Nat. Commun.* **2016**, *7*, 13461.
[44] I. Gadwal, G. Sheng, R. L. Thankamony, Y. Liu, H. F. Li, Z. P. Lai, *ACS Appl. Mater. Interfaces* **2018**, *10*, 12295–12299.
[45] Q. Hao, C. Q. Zhao, B. Sun, C. Lu, J. Liu, M. J. Liu, L. J. Wan, D. Wang, *J. Am. Chem. Soc.* **2018**, *140*, 12152–12158.
[46] Y. Chen, M. Li, P. Payamyar, Z. Zheng, J. Sakamoto, A. D. Schlüter, *ACS Macro Lett.* **2014**, *3*, 153–158.
[47] V. Müller, F. Shao, M. Baljozovic, M. Moradi, Y. Zhang, T. Jung, W. B. Thompson, B. T. King, R. Zenobi, A. D. Schlüter, *Angew. Chem. Int. Ed.* **2017**, *56*, 15262–15266.
[48] P. Payamyar, M. Servalli, T. Hungerland, A. P. Schütz, Z. Zheng, A. Borgschulte, A. D. Schlüter, *Macromol. Rapid Commun.* **2015**, *36*, 151–158.
[49] X. N. Kan, Y. Q. Ban, C. Y. Wu, Q. Y. Pan, H. Liu, J. H. Song, Z. C. Zuo, Z. B. Li, Y. J. Zhao, *ACS Appl. Mater. Interfaces* **2018**, *10*, 53–58.
[50] R. Matsuoka, R. Sakamoto, K. Hoshiko, S. Sasaki, H. Masunaga, K. Nagashio, H. Nishihara, *J. Am. Chem. Soc.* **2017**, *139*, 3145–3152.
[51] Q. Y. Pan, H. Liu, Y. J. Zhao, S. Q. Chen, B. Xue, X. N. Kan, X. W. Huang, J. Liu, Z. B. Li, *ACS Appl. Mater. Interfaces* **2019**, *11*, 2740–2744.
[52] K. Ariga, M. Matsumoto, T. Mori, L. K. Shrestha, *Beilstein J. Nanotechnology* **2019**, *10*, 1559–1587.
[53] K. Ariga, S. Watanabe, T. Mori, J. Takeya, *NPG Asia Mater.* **2018**, *10*, 90–106.
[54] X. Y. Jin, N. Song, X. Wang, C. Y. Wang, Y. Wang, Y. W. Yang, *Sci. Rep.* **2018**, *8*, 4035.
[55] J. Mei, Y. Hong, J. W. Lam, A. Qin, Y. Tang, B. Z. Tang, *Adv. Mater.* **2014**, *26*, 5429–5479.
[56] J. Mei, N. L. Leung, R. T. Kwok, J. W. Lam, B. Z. Tang, *Chem. Rev.* **2015**, *115*, 11718–11940.
[57] X. H. Wang, N. Song, W. Hou, C. Y. Wang, Y. Wang, J. Tang, Y. W. Yang, *Adv. Mater.* **2019**, *31*, 1903962.
[58] C. Liu, Y. Hang, T. Jiang, J. Yang, X. Zhang, J. Hua, *Talanta* **2018**, *178*, 847–853.
[59] L. Tang, H. Yu, K. Zhong, X. Gao, J. Li, *RSC Adv.* **2019**, *9*, 23316–23323.
[60] Y. Liu, Y. Yu, J. W. Lam, Y. Hong, M. Faisal, W. Z. Yuan, B. Z. Tang, *Chem. Eur. J.* **2010**, *16*, 8433–8438.
[61] Y. Hou, J. Du, J. Hou, P. Shi, K. Wang, S. Zhang, T. Han, Z. Li, *Dyes Pigm.* **2019**, *160*, 830–838.
[62] F. Tang, J. Peng, R. Liu, C. Yao, X. Xu, L. Li, *RSC Adv.* **2015**, *5*, 71419–71424.
[63] H. Zhang, J. Zeng, W. Luo, H. Wu, C. Zeng, K. Zhang, W. Feng, Z. Wang, Z. Zhao, B. Z. Tang, *J. Mater. Chem. C* **2019**, *7*, 6359–6368.
[64] L. Ascherl, T. Sick, J. T. Margraf, S. H. Lapidus, M. Calik, C. Hettstedt, K. Karaghiosoff, M. Döblinger, T. Clark, K. W. Chapman, F. Auras, T. Bein, *Nat. Chem.* **2016**, *8*, 310–316.
[65] F. Z. Cui, J. J. Xie, S. Y. Jiang, S. X. Gan, D. L. Ma, R. R. Liang, G. F. Jiang, X. Zhao, *Chem. Commun.* **2019**, *55*, 4550–4553.
[66] L. Ma, X. Feng, S. Wang, B. Wang, *Mater. Chem. Front.* **2017**, *1*, 2474–2486.
[67] T. Y. Zhou, S. Q. Xu, Q. Wen, Z. F. Pang, X. Zhao, *J. Am. Chem. Soc.* **2014**, *136*, 15885–15888.
[68] H. Liu, Q. Pan, C. Wu, J. Sun, T. Zhuang, T. Liang, X. Mu, X. Zhou, Z. Li, Y. Zhao, *Mater. Chem. Front.* **2019**, *3*, 1532–1537.
[69] S. Dalapati, E. Jin, M. Addicoat, T. Heine, D. Jiang, *J. Am. Chem. Soc.* **2016**, *138*, 5797–5800.
[70] L. Opilik, P. Payamyar, J. Szczerbinski, A. P. Schütz, M. Servalli, T. Hungerland, A. D. Schlüter, R. Zenobi, *ACS Nano* **2015**, *9*, 4252–4259.
[71] F. Shao, W. Dai, Y. Zhang, W. Zhang, A. D. Schlüter, R. Zenobi, *ACS Nano* **2018**, *12*, 5021–5029.
[72] F. Shao, V. Müller, Y. Zhang, A. D. Schluter, R. Zenobi, *Angew. Chem. Int. Ed.* **2017**, *56*, 9361–9366.
[73] T. Bauer, Z. Zheng, A. Renn, R. Enning, A. Stemmer, J. Sakamoto, A. D. Schlüter, *Angew. Chem. Int. Ed.* **2011**, *50*, 7879–7884.
[74] B. S. Y. W. Zhang, T. Schmid, R. Zenobi, *J. Phys. Chem. C* **2007**, *111*, 1733–1738.
[75] T. S. W. Zhang, B. Slang, R. Zenob, *Isr. J. Chem.* **2006**, *47*, 177–184.

Manuscript received: February 13, 2020
Revised manuscript received: February 21, 2020